Proceedings of ASME Turbo Expo 2015: Power for Land, Sea and Air
ASME 2015
June nn-nn, 2015, Montreal, Canada

GT2015-42736

ADJOINT SENSITIVITY ANALYSIS OF HYDRODYNAMIC STABILITY IN A GAS TURBINE FUEL INJECTOR

Outi Tammisola

Department of Mech., Materials and Manuf. Engineering
University of Nottingham
University Park, Coates building
NG72RD, United Kingdom
Email: Outi-leena.tammisola@nottingham.ac.uk

Matthew P. Juniper *

Engineering Department
University of Cambridge
Trumpington Street, Cambridge,
CB2 1PZ, United Kingdom
Email: mpj1001@cam.ac.uk

ABSTRACT

Hydrodynamic oscillations in gas turbine fuel injectors help to mix the fuel and air but can also contribute to thermoacoustic instability. Small changes to some parts of a fuel injector greatly affect the frequency and amplitude of these oscillations. These regions can be identified efficiently with adjoint-based sensitivity analysis. This is a linear technique that identifies the region of the flow that causes the oscillation, the regions of the flow that are most sensitive to external forcing, and the regions of the flow that, when altered, have most influence on the oscillation. In this paper, we extend this to the flow from a gas turbine's single stream radial swirler, which has been extensively studied experimentally (GT2008-50278) [8].

The swirling annular flow enters the combustion chamber and expands to the chamber walls, forming a conical recirculation zone along the centreline and an annular recirculation zone in the upstream corner. In this study, the steady base flow and the stability analysis are calculated at Re 200-3800 based on the mean flow velocity and inlet diameter. The velocity field is similar to that found from experiments and LES, and the local stability results are close to those at higher Re (GT2012-68253) [11].

All the analyses (experiments, LES, uRANS, local stability, and the global stability in this paper) show that a helical motion develops around the central recirculation zone. This develops into a precessing vortex core. The adjoint-based sensitivity analysis reveals that the frequency and growth rate of the oscillation is dictated by conditions just upstream of the central recirculation zone (the wavemaker region). It also reveals that this oscillation is very receptive to forcing at the sharp edges of the injector. In practical situations, this forcing could arise from an impinging acoustic wave, showing that these edges could be influential in the feedback mechanism that causes thermoacoustic instability.

The analysis also shows how the growth rate and frequency of the oscillation change with either small shape changes of the nozzle, or additional suction or blowing at the walls of the injector. It reveals that the oscillations originate in a very localized region at the entry to the combustion chamber, which lies near the separation point at the outer inlet, and extends to the outlet of the inner pipe. Any scheme designed to control the frequency and amplitude of the oscillation only needs to change the flow in this localized region.

NOMENCLATURE

- D characteristic lengthscale
- f frequency (Hz)
- i $\sqrt{-1}$
- m azimuthal wavenumber (real integer)
- p pressure field
- $\hat{p}$ pressure profile in the axial-radial plane

*Address all correspondence to this author.

$\hat{q}$ state vector, $\hat{q} \equiv (\hat{\mathbf{u}}, \hat{p})^T$
r radial coordinate
Re Reynolds number
St Strouhal number, $\mathrm{St} \equiv fD/U$ (complex)
St_i non-dimensional temporal growth rate
St_r non-dimensional frequency
t time
U characteristic velocity
u axial velocity
$\mathbf{u}$ velocity field, $\mathbf{u} \equiv (u, v, w)^T$
$\hat{\mathbf{u}}$ velocity profile in the axial-radial plane
v radial velocity
w azimuthal velocity
x axial coordinate

Greek:

θ azimuthal coordinate
ω_i global temporal growth rate
ω_r global temporal angular frequency
ω global angular frequency (complex)

Superscripts:

$'$ direct perturbation
$+$ adjoint perturbation

Subscripts:

g global
i imaginary
r real

INTRODUCTION

This paper outlines a methodology for the analysis and control of hydrodynamic instabilities occurring in combustor flows. It is demonstrated on a non-reacting flow through a gas turbine fuel injector, following a case that has already been extensively studied numerically and experimentally. The analysis detects the regions of the flow that most influence the formation of the instability and identifies modifications to the flow that can eliminate or enhance the instability. The calculated sensitivities to velocity and pressure forcing reveal the response of the instability mode to acoustic forcing. This may aid understanding of the flame's transfer function and thermoacoustic instability. It is demonstrated here on a flow calculated with DNS at moderate Reynolds number so that the results of the stability analysis can be rigorously compared with the DNS results. However, its main benefit to engineers will be in its application to the post-processing of LES, uRANS, RANS, or experimental data, which is equally feasible.

The flow in a gas turbine combustion chamber has to achieve a high heat release rate while keeping the flame stabilized. This is usually achieved by swirling the air flow such that a vortex breakdown bubble forms just downstream of the injector [1]. This ensures that hot products recirculate in the bubble and come into contact with the cold reactants. It also ensures that the flow is strongly hydrodynamically unstable. This instability causes large scale coherent structures to form, which rapidly mix the fuel and air and achieve high energy densities [2].

These large scale coherent structures form from the nonlinear development of large scale linear instabilities. One example is the precessing vortex core (PVC) that is often found in swirl injectors. This is the nonlinear development of a helical mode, the outcome of which is, for example, clearly seen in the flow around a vortex breakdown bubble at a Reynolds number around 100 [3–5]. At this Reynolds number, viscous damping hinders the growth of higher modes and the transition to turbulence, which are observed in combustion chambers. The PVC is not observed in all flows and is more prevalent in non-reacting flows than in reacting flows. Its existence is known to be sensitive to the density profiles and to the way that the air is injected [6]. For example, if a small amount of air is injected along the centreline of the vortex breakdown bubble, the vortex core stops precessing [7, 8]. The methodology in this paper calculates linear instabilities and assesses their sensitivity to changes in the flow, such as those described above.

Previous hydrodynamic stability analysis of this type of flow has involved local stability analysis [9–11]. The local analysis examines each axial position separately by assuming that the flow is locally parallel there. This assumption is clearly violated in this flow. Nevertheless, local stability analysis has proven to be very useful for the physical understanding of hydrodynamic instability in this flow. It has shown that the core of the instability (the wavemaker region) of the single helical mode and the double helical mode is in the upstream region of the flow [11]. Furthermore, the structures found from the local stability analysis, which is linear, have been found to match those extracted from Proper Orthogonal Decomposition of experimental data in a case where the flow is reasonably parallel [10]. Local analysis has been used for the study of industrial gas turbine fuel injectors and, because it is computationally cheap and robust, will probably continue to be used for this.

Global stability analysis, which is the subject of this paper, does not assume that the flow is locally parallel. It is therefore more appropriate for the study of hydrodynamic stability in gas turbine combustion chambers. A useful guide for the methodology in this paper is given by the results for a vortex breakdown bubble at $\mathrm{Re} = 100$, for which a global stability analysis and adjoint sensitivity analysis has been performed [5]. In that study,

the adjoint global modes reveal the regions of the flow that are most receptive to external forcing [13], and also the wavemaker of the oscillation [14, 15]. This type of analysis can also give the sensitivity to steady forcing of the base flow [16, 17]. Global stability analysis is rigorously valid when it is applied around a steady (but possibly unstable) laminar flow. It also works well when applied around a time-averaged mean flow [18] and to flows at high Reynolds numbers [19]. The applicability of linear stability analysis, particularly when applied around a turbulent mean flow, is still an area of active research. A detailed review of the theoretical background and existing research can be found in the introduction of Ref. [19].

Section 1 describes the technique used in this paper. Section 2 starts by describing the flow, its mean, and its most energetic POD modes. Then the linear stability analysis is performed on the mean flow and its predictions are compared with the POD modes in order to test the suitability of the linear analysis. Section 3 describes the adjoint global mode and its physical interpretation, as well as the wavemaker region of this flow, and its sensitivity to steady forcing. Finally, section 4 presents techniques that will be useful for injector design, such as the sensitivity to changes in the injector shape. The results in section 4 are at a lower Reynolds number than those in sections 1 to 3, and the main interest is the technique rather than the result itself. The overall aim of the paper is to show the relevance of these techniques to the design of gas turbine fuel injectors.

1 Methodology and numerical methods

The characteristic variables are the inflow velocity at the swirler inlet, U_0, the swirl velocity at the swirler inlet, W_0, the swirler exit radius $R_{sw,out}$, and the density and molecular viscosity of air. This gives Reynolds number $Re = (\rho U_0 R_{sw,out}/\mu) = 1250$ and Swirl number $Sw = W_0/U_0 = 0.5$. (If the combustor entry quantities are used instead, $Re_{entry} = 3900$ and $Sw_{entry} = 1.3$).

There are four stages to the methodology in this paper. Of these, the first stage (DNS) and the second stage (POD) are not part of the global stability analysis, which starts at the third stage. They are included so that the linear results can be rigorously compared with nonlinear results. It is equally possible to apply the third and fourth stages to LES, uRANS, RANS, or experimentally-derived results.

In the first stage, the Nek5000 code [20, 21] is used for direct time integration of the 3D nonlinear incompressible Navier–Stokes equations. The computational grid has 58720 spectral elements of order $p = 6$, giving 8.8×10^6 degrees of freedom. The Nek5000 is based on a spectral element method (SEM) [22], combining the high-order accuracy of spectral methods with the geometrical flexibility of finite element methods (FEM). The time advancement is performed using a semi-implicit 2^{nd} order backwards differentiation-extrapolation scheme. Grid sensitivity studies have been performed with half the number of elements on both nonlinear and linear results in this paper, to confirm the grid independency of linear and nonlinear frequencies. The Reynolds number is set to 1250, which is large enough for the flow to have turbulent features similar to those in the LES of [8] but small enough to be numerically tractable. Figure 1 shows a snapshot of the axial velocity of the flow.

In the second stage, we extract proper orthogonal decomposition (POD) modes from the DNS data. POD is a statistically based method to extract the most energetic structures from numerical or experimental data [23]. In fluid mechanics, POD is applied with the purpose of extracting large-scale coherent structures from unsteady or turbulent time-dependent simulation data because the large-scale structures are often (but not always) the ones with the highest energies. To find the POD modes, the mean flow is first subtracted from the nonlinear time series. The POD modes are computed by a singular value decomposition of the snapshot matrix [24] in Matlab. In this paper, we compute the POD modes in order to compare them with the global modes, calculated in the third stage of the analysis.

In the third stage, the base flow is formed by taking the time average of the 3D DNS data. Here, it is worth emphasizing that the mean flow could be obtained computationally more cheaply by RANS, LES, or even experiments. The mean flow is averaged in the azimuthal direction to obtain an axisymmetric base flow. We then examine the evolution of infinitesimal three-dimensional unsteady perturbations about this mean flow. To do this, the Navier–Stokes equations are linearized around the base flow to obtain

$$\begin{aligned} \frac{\partial \mathbf{u}}{\partial t} + \mathbf{u}\cdot\nabla\mathbf{U}_b + \mathbf{U}_b\cdot\nabla\mathbf{u} &= -\nabla\hat{p} + \nabla\cdot\left[Re_{eff}^{-1}(\nabla\mathbf{u} + \nabla\mathbf{u}^T)\right] \\ \nabla\cdot\mathbf{u} &= 0, \end{aligned} \tag{1}$$

where we have employed the Newtonian eddy model [25] and introduced the spatially varying turbulent *effective Reynolds number*

$$Re_{eff} = \frac{\rho U_0 R_0}{\mu + \mu_t} = Re\left(\frac{\mu}{\mu + \mu_t}\right), \tag{2}$$

where μ_t is the turbulent viscosity extracted from the nonlinear simulation data as a ratio between turbulent energy production and mean flow dissipation (in tensor notation):

$$\mu_t = \frac{-\rho\overline{u_i' u_j'}\frac{\partial \overline{U}_i}{\partial x_j}}{\overline{S_{ij}}\,\overline{S_{ij}}}, \tag{3}$$

and $\overline{S_{ij}}$ is the dimensional mean flow viscous stress tensor. Before computing the turbulent viscosity, the coherent motions were subtracted from the DNS data as described in Sec. 2.

By applying the Newtonian eddy model, we assume that the coherent motions are affected by the local mean flow Reynolds stresses, but the Reynolds stresses in turn are not affected by the coherent motions. This approach assumes a separation of scales, and a relatively low amplitude of the coherent motions. Perturbation of the Reynolds stresses would require a model for them. This approach is selected primarily because it allows us to extract the mean flow Reynolds stresses from the nonlinear simulation data as the ratio between turbulent energy production and mean flow dissipation:

The base flow is axisymmetric and the analysis is linear, so the perturbation can be expressed as the sum of azimuthal modes of the form $\exp(\sigma t + \mathrm{i}m\theta)$, and each azimuthal mode, m, can be considered independently. In this study, we find that $m = 1$ and $m = 2$ are the most unstable modes, so we focus only on these. The frequency of each mode is given by $Im(\sigma)$ and its growth rate by $Re(\sigma)$. Where the global modes are calculated with eddy viscosity, they are obtained with finite element (FEM) software FreeFem++ [26], where UMFPACK is used for the solution of linear systems and ARPACK for eigenvalue computation. We have derived and implemented the variational form of (1) with the above azimuthal mode Ansatz.

In the fourth stage, we obtain the adjoint global modes in a similar manner to the direct global modes, by solving the adjoint equation of (1):

$$\begin{aligned} -\sigma\mathbf{u}^{+} - \nabla\mathbf{U}_b\cdot\mathbf{u}^{+} + \mathbf{U}_b\cdot\nabla\mathbf{u}^{+} &= -\nabla p^{+} - \nabla\cdot\left[Re_{eff}^{-1}\left(\nabla\mathbf{u}^{+} + \nabla\mathbf{u}^{+T}\right)\right] \\ \nabla\cdot\mathbf{u}^{+} &= 0, \end{aligned} \tag{4}$$

With one additional computation, the direct and adjoint global modes can be combined to estimate the effect of changes in the flow field, or injector boundaries, on the formation of hydrodynamic instability, as will be shown in Sec. 3.

2 POD and Direct global modes

The flow through the injector is calculated at Re = 1250. Snapshots of the axial velocity are shown in figure 1. The flow is laminar in the injector nozzle until the separation point on the inner wall, which is the upstream end of the recirculation bubble. The strong axial and azimuthal shear between the recirculation bubble and the outer stream generate Kelvin-Helmholtz instabilities that grow into large vortical structures, which convect downstream. Probes of the three velocity components placed in the flow show a clear spectral peak at $St = 0.69$ and a small peak at $St = 1.5$. These are caused by coherent structures in the flow. The first value is exactly the same as that found for this injector using experiments [7] and LES [8].

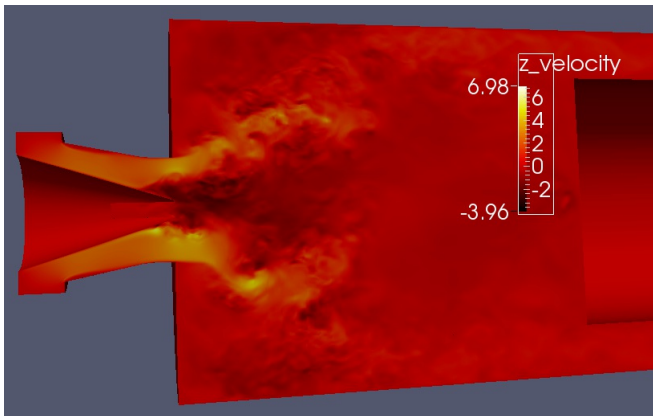

(a)

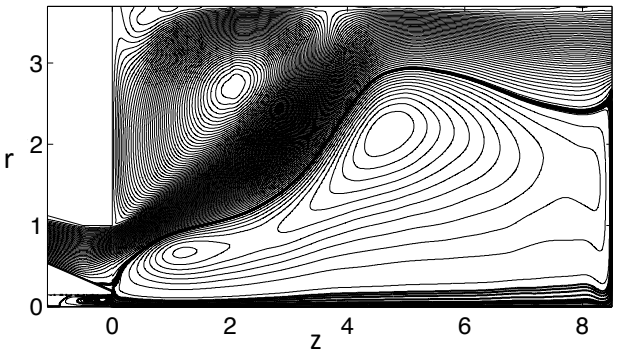

(b)

FIGURE 1: (a) Instantaneous axial velocity of the flow through the injector. Light colors indicate positive axial velocity (maximum = +6.98) and dark colours indicate negative axial velocity (minimum = −3.96). (b) Streamlines of the mean flow in the axial-radial plane.

.

The shape of these structures is difficult to see from these snapshots but is revealed clearly by performing the Proper Orthogonal Decomposition (POD) on snapshots of the DNS. Figure 2 shows POD mode 1 (left) and POD mode 3 (right). Modes 2 and 4 are similar to 1 and 3 but are $\pi/4$ out of phase. The first POD pair (1&2) account for 17.9% of the total energy. The second POD pair (3&4) account for 5.4%. The top frames show 3D contours of the axial velocity, as viewed from the injection plane. This shows that mode 1 is a single helix motion while mode 3 is a double helix. The precession of the vortex core causes the motion seen in POD mode 1. Both modes have been observed in experiments [7] and LES [8] of this injector. Having observed from the 3D POD modes that the most energetic modes have azimuthal wavenumber $m = 1$ and $m = 2$, we filter them by a Fourier decomposition in the azimuthal direction, where only the dominant Fourier component ($m = 1$ for mode 1-2, and $m = 2$ for mode

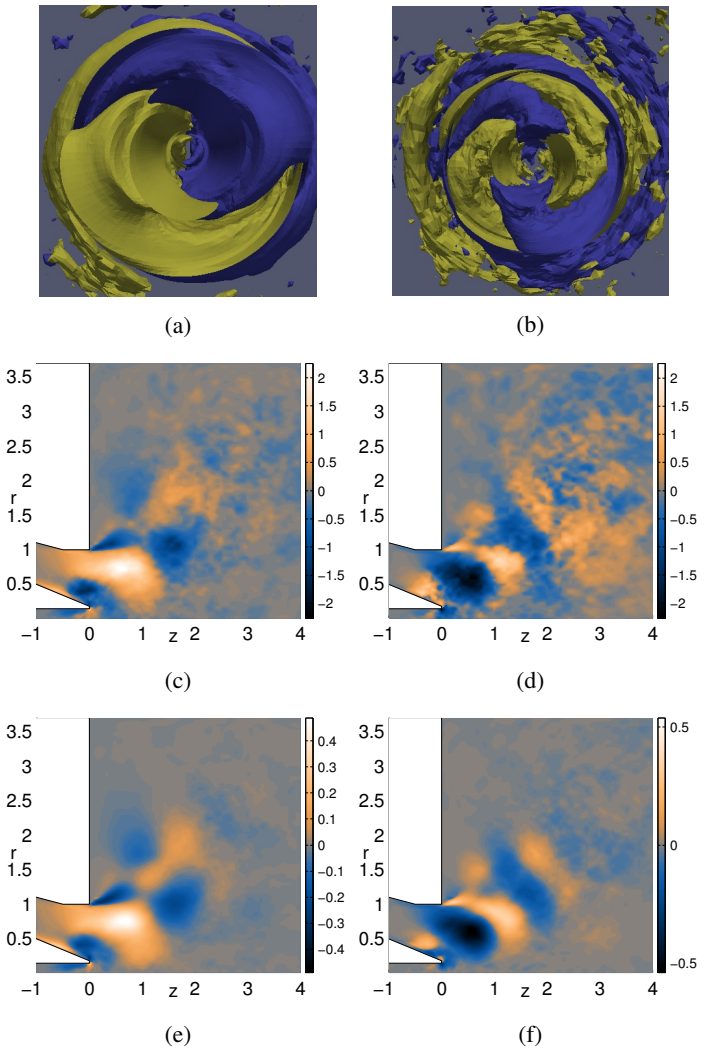

FIGURE 2: Left column: POD mode 1. Right column: POD mode 3. Top row: 3D iso-surfaces of axial velocity: blue (negative) and yellow (positive). Middle row: contours of axial velocity at one azimuthal location. Bottom row: contours of axial velocity averaged in the azimuthal direction.

3-4) is kept. This increases the amount of available information for the calculation of each POD mode and makes the resulting POD modes smoother (bottom frames of figure 2).

The POD modes described above were calculated with a long time interval between adjacent snapshots. A second POD analysis was performed with 261 closely-spaced snapshots in order to extract the frequencies of modes 1 and 2. This gives $St = 0.70 \pm 0.06$ for the $m = 1$ mode and $St = 1.47 \pm 0.06$ for the $m = 2$ mode. This confirms that the smaller peak observed in the probe signal does indeed come from the $m = 2$ mode.

The velocity field from the DNS is time-averaged. Streamlines of the axial and radial velocity components are shown in figure 1(b). These streamlines are very similar to the streamlines of time-averaged LES shown in figure 5 of [8]. There are two large recirculation zones within the combustor, which is characteristic of swirl injectors [30]. This is the base flow on which we perform a linear stability analysis to extract the linear direct and adjoint global modes.

The linear global modes can be estimated from equation (1) using molecular viscosity. The physical justification for this is that, at high Reynolds number, viscous forces do not play a primary role in the driving mechanism, mode selection, and frequency selection of this instability. Nevertheless, a more accurate calculation of the linear global modes is obtained by using non-uniform eddy viscosity in equation (1), particularly if the effective Reynolds number falls below $\mathrm{Re} = 100$, as for Reynolds numbers in this regime viscosity has significant effect on the hydrodynamic instability [31]. This approach was suggested, but not implemented, by [19]. The same principle was used to model the effect of eddy viscosity on aeroacoustic interactions in [28], but there the turbulent viscosity was determined from a LES subgrid scale model. We extract the eddy viscosity by assuming that the large scale coherent structures are predominantly in POD modes 1&2 and 3&4. We subtract these POD modes from the original time series and then compute the Reynolds stresses of the resulting flow in order to calculate the eddy viscosity. This can be expressed as a spatially-varying Reynolds number, which is shown in figure 3. This Reynolds number is small (i.e. the eddy viscosity is large) in regions in which the fluctuations are large, for example in the shear layer between the injected flow and the central recirculation zone. It is large (the eddy viscosity is small) in the inlet flow and near the walls. Its value in much of the combustion chamber is $\mathrm{Re}_{eff} < 100$, which is sufficiently low that it has appreciable influence on the stability of the flow.

The direct global modes are then calculated using this effective Reynolds number. For the first azimuthal mode ($m = 1$), the resulting direct global mode is shown in the left frames of figure 4 with the corresponding POD mode on the right frames of figure 4. This is the precessing vortex core (PVC). The second azimuthal mode ($m = 2$) is shown similarly in figure 5. This is a double-helical mode.

There is exceptionally good agreement between the direct global modes and their corresponding POD modes, considering that the two methods are so different. It is worth exploring the ramifications of this. On the one hand, the POD modes are extracted directly from DNS snapshots. Beyond this extraction, there are no further calculations, and they are therefore a faithful representation of the most energetic motions in the fully developed nonlinear turbulent flow. On the other hand, the direct global modes are calculated (i) by extracting the mean flow and frozen eddy viscosity from the DNS data and then (ii) calculating the shape and frequency of infinitesimal perturbations that would grow on top of this flow, given that eddy viscosity. This involves

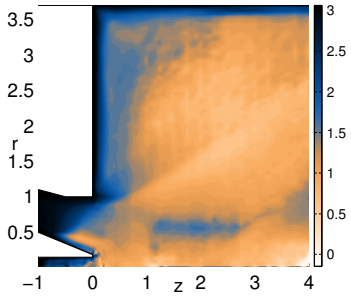

FIGURE 3: Log (base 10) of the effective turbulent Reynolds number in the axial–radial plane obtained from the DNS after subtraction of the POD modes in figure 2

a somewhat artificial calculation: a linear stability analysis on a turbulent mean flow. Nevertheless, the fact that the direct global modes are so close to the POD modes shows that the mode shape and frequency of the oscillation can be predicted just from linear stability analysis around mean flow quantities [19]. In other words, during the nonlinear saturation of this mode, its characteristics change very little from those predicted at infinitesimal amplitude. This has particularly powerful consequences because a linear stability analysis around mean flow quantities can generate much more information than just the direct global mode shown so far in this paper. This information, which is the subject of the rest of this paper, is not accessible by post-processing techniques such as the POD.

3 Adjoint global modes, receptivity, and sensitivity

Figure 6(a–c) shows the adjoint global mode of the first helical ($m = 1$) mode, the PVC, at $Re = 1250$. Although the sensitivities of the second double-helical ($m = 2$) mode have also been computed, in this paper we only demonstrate the sensitivities on the more well-known PVC mode. The review article by Chomaz [13] on global instabilities in spatially-developing flows permits a physical understanding of the adjoint global mode. The adjoint global mode determines how a global mode (such as the PVC in this paper) would respond to external periodic forcing. If the flow is externally forced in regions in which the adjoint global mode has high amplitude then a subcritical PVC will respond strongly and grow to a large amplitude. The different components of the adjoint global mode reveals that the locations of high receptivity of the PVC depend on the type of forcing. Figure 6(a–b) shows the receptivity to volume forcing – i.e. a forcing mechanism that enters into the momentum equations. Figure 6(c) shows the receptivity to local compressibility/dilation – i.e. a forcing mechanism that enters into the continuity equation. It is interesting to consider how an acoustic wave impinging on the injector would force the flow because it is clear that this mode

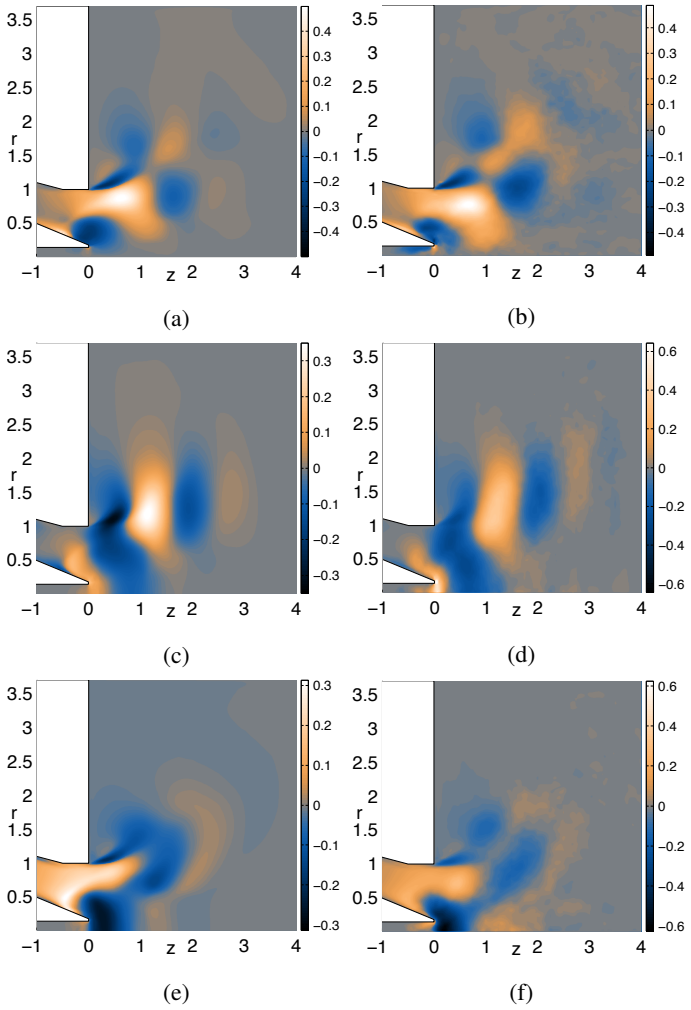

FIGURE 4: Left column: the most unstable global mode with azimuthal wavenumber $m = 1$ (the single helix mode). This is calculated with the linear global analysis around the mean flow with the effective Reynolds number shown in figure 3. Right column: the first POD mode (the left column of figure 2). This is extracted from the DNS. Top row: axial velocity ($\hat{u}$). Middle row: radial velocity ($\hat{v}$). Bottom row: azimuthal velocity ($\hat{w}$). There is excellent agreement, showing that the linear analysis around the mean flow captures the same features that are observed in the nonlinear DNS.

($m = 1$) is most receptive to all types of forcing around the sharp corners of the injector. In a combustion chamber, acoustic oscillations provoke hydrodynamic convective instabilities in the flame, which then cause heat release fluctuations some time later. If the heat release perturbations occur during times of higher acoustic pressure, this increases the amplitude of acoustic oscillations. In a calculation involving this mechanism, it is likely

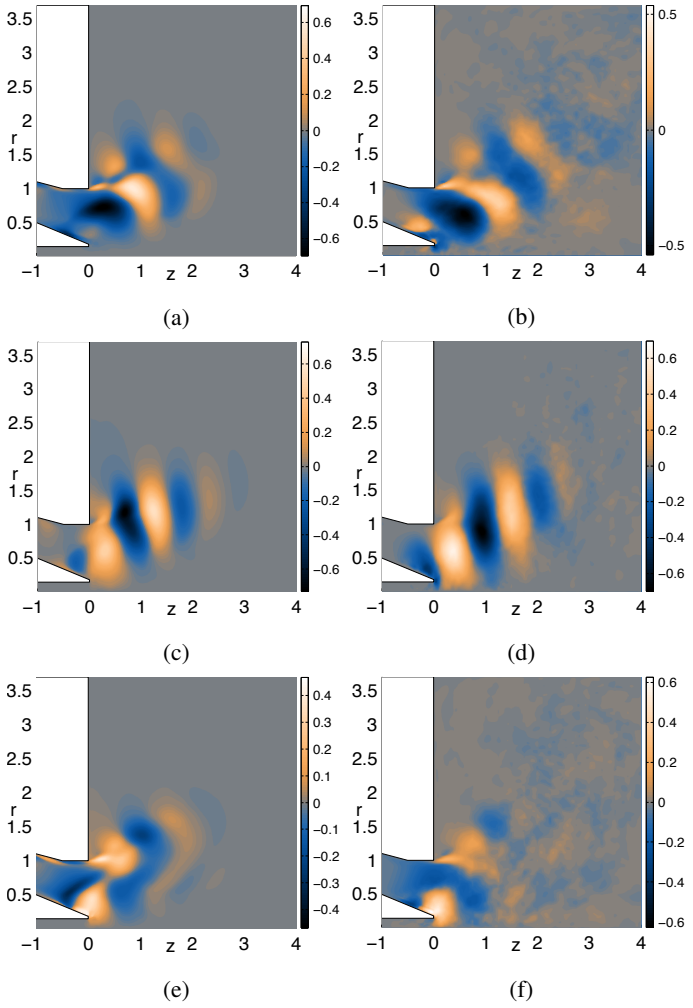

FIGURE 5: As for figure 4 but for azimuthal wavenumber $m = 2$ (the double helix mode) and for the third POD mode (the right column of figure 2).

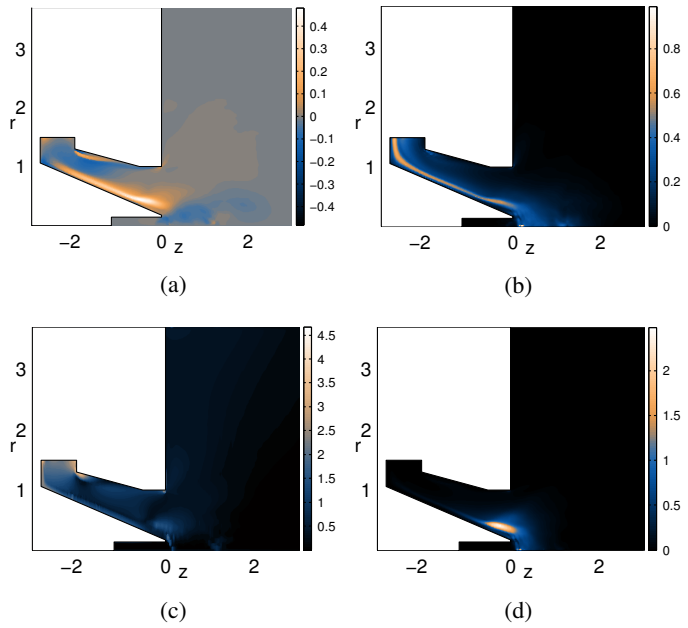

FIGURE 6: (a) Receptivity to volume forcing in the axial direction ($Re(u^+)$). (b) Receptivity to volume forcing, magnitude ($|\mathbf{u}^+|$). (c) Receptivity to local compressibility ($|p^+|$). (d) Structural sensitivity ($|\mathbf{u}^{*+} \cdot \mathbf{u}|$).

that the corners of the injector will be very influential. This is an area of current study [32].

Figure 6(d) shows the overlap between the direct and adjoint global modes of the first helical ($m = 1$) mode. This also has a physical meaning.Changes to the flow in regions where this overlap has high amplitude will have most influence on the mode growth rate. In other words, where the overlap is high, small changes have the greatest chance to suppress the growth of PVC. This is therefore interpreted as the 'wavemaker' region of the flow, i.e. the region of the flow that drives the oscillation, while the rest of the flow merely responds to driving from the wavemaker region. In this case, the wavemaker region lies just upstream of the inner recirculation zone, near the separation point along the central injector. The same result was found by [5] for the flow around a vortex breakdown bubble at Re = 100. That paper also examined the components of the overlap between direct and adjoint global modes to reveal the origins of the instability, which is predominantly a Kelvin-Helmholtz mechanism in the shear layer around the upstream part of the recirculation bubble.

This direct/adjoint global mode analysis reveals that the region of the flow that makes the vortex core precess lies just upstream of the vortex breakdown bubble. This implies that small changes to the flow in this region will have a particularly strong influence on the growth rate and frequency of the precessing motion and shows which part of the flow should be altered in order to control the precessing vortex core.

4 Base flow sensitivity at low Reynolds number

Adjoint-based sensitivity analysis will be particularly useful if it can be used in injector design. Here, we demonstrate some outcomes of adjoint-based sensitivity that could be useful. We have performed these at low Reynolds number (Re = 68) for this injector but in future work the techniques will be extended to stability analysis around the mean flow.

Figure 7 shows the base flow at Re = 68. The direct and adjoint modes are found from equations (1) and (4), as before, but using molecular viscosity rather than eddy viscosity because the flow is laminar. The first helical ($m = 1$) mode is marginally un-

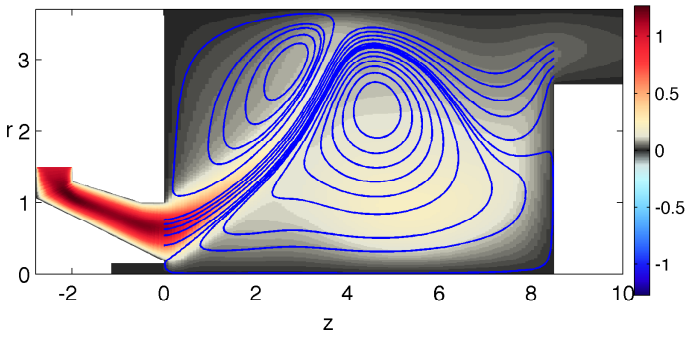

FIGURE 7: The laminar flow in the same geometry at Re = 68, used as a base flow for the low Reynolds number calculations. The azimuthal velocity is shown in color and streamlines in the axial-radial plane are shown as lines.

stable. Figure 8 shows the sensitivity of this mode to momentum forcing in the axial, radial, and azimuthal directions. Although this forcing would usually be difficult to enact, it gives useful physical insight into mechanisms that will enhance or reduce instability. For example, the blue region in figure 8(top) shows that axial momentum forcing in the downstream direction just downstream of the central injector will greatly stabilize the $m = 1$ mode. This is analogous to the stabilizing effect of base bleed behind cylinders found by [16] using these techniques. This helps to explain a result in the study of [8] in which it was shown that the $m = 1$ mode was stabilized by injection of air down the central jet.

Figure 9 (a) shows the sensitivity of this mode to changes of inflow velocity to the domain. At the walls, a negative value of the sensitivity means that the mode would be stabilized by mass injection/blowing, which means inflow at the walls, whereas a positive value means that the mode would be destabilized by mass injection/blowing. Figure 9(a) shows that the $m = 1$ mode would be slightly stabilized by blowing through the boundaries of the outer duct, particularly if the blowing were towards the tip of the injector.

However, this figure shows that the most influential stabilization is achieved by blowing through the inner duct (adding a central jet). Physically, this is the same result as that shown in figure 8. The sensitivity to swirl (tangential velocity) has also been investigated (although not shown here), with the result that increasing swirl at the swirler inlet or near the swirler tip promotes the precessing vortex core, while adding swirl to other boundaries has no effect.

For injector designers, the most practical type of sensitivity is the sensitivity to modification of the shape of the boundary. This is shown in figure 9 (b). This result shows that the largest sensitivity to shape variations is at two of the corners of the outer inlet. The colors show the effect of outwards movement of the

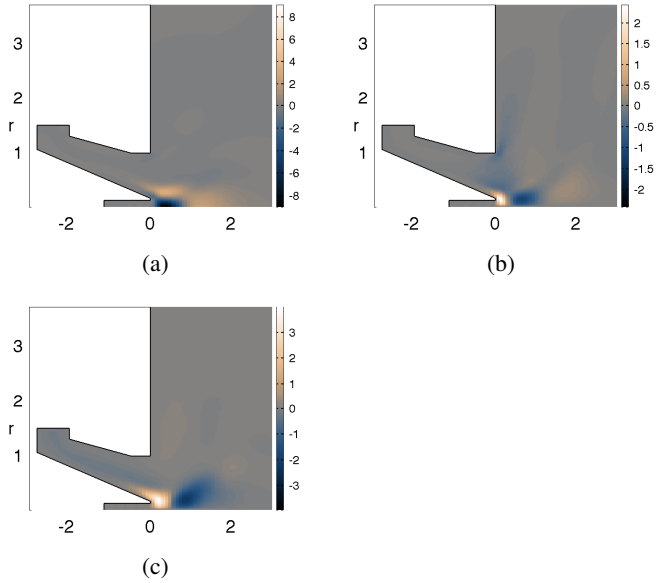

FIGURE 8: Sensitivity to a steady volume force at Re = 68, (a) axial force, (b) radial force, (c) azimuthal force. The colors show the influence of a local unit force in the positive (a) axial, (b) radial, (c) azimuthal directions. Positive values indicate that the force is destabilizing. Negative values indicate that the force is stabilizing.

boundary. Near the tip of the injector, this shows that, in order to stabilize the flow, the inner pipe wall should be moved down and the horizontal part between the two inlets should be moved upstream. Both changes would contribute to a more rounded shape of this corner. The sensitivity is also high in the downstream corner near the swirler inlet. According to the sensitivity, this corner should be moved inwards to stabilize the flow.

5 CONCLUSIONS

Adjoint sensitivity analysis has become an increasingly common tool in the study of flows near the onset of instability. This linear technique reveals how the stability of a flow is altered when small changes are made to the flow. Once the direct and adjoint global modes have been calculated, the influence of any linear feedback mechanism or any small perturbation to the base flow can be calculated with one small calculation. Consequently, it is a general method that has intriguing practical applications.

This method was applied initially to canonical flows, such as the flow around a cylinder. Increasingly complex and high Reynolds number flows have now been examined with adjoint sensitivity analysis, such as the flow over an airfoil at a Mach number of 0.85 [19]. High Reynolds number flows are invariably turbulent. Nevertheless, many exhibit long wavelength low

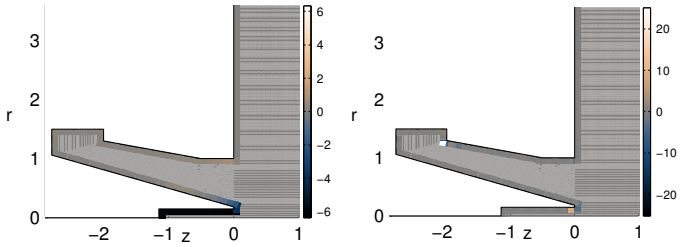

FIGURE 9: (a) Sensitivity to inflow at the domain boundaries at $\mathrm{Re} = 68$. (The sensitivity is shown for both wall boundaries (where inflow means blowing/injection) and inflow boundaries (where inflow means an increasing inflow velocity). This shows that inflow in the inner channel and at the wall near the separation point is stabilizing. (b) Sensitivity to outwards movement of the domain boundary (shape sensitivity). This shows that changes at two of the corners are influential.

frequency oscillations, which are amenable to adjoint sensitivity analysis. The analysis has to be performed around a mean flow, however, which is not yet rigorously justified. Even so, linear stability analysis applied around mean flows gives results that are similar to those extracted from nonlinear simulations, lending weight to the argument that these results are useful from an engineering point of view, even if a rigorous justification is not yet available.

In this paper, we present adjoint sensitivity analysis of the flow in a fuel injector that has already been extensively studied. The analysis is performed around the mean flow taken from DNS. Firstly, the two most unstable linear global modes are compared with the first and second POD modes, which are also extracted from the DNS. The comparison is excellent, showing that the linear global analysis performed around the mean flow produces the same features that are observed in the fully nonlinear DNS. Secondly, the corresponding adjoint global modes are calculated. These are shown here for the first helical mode, which causes the precessing vortex core that is often observed in combustion chambers. This reveals the regions in which the flow is most receptive to external forcing. This shows that the flow is only receptive around the injector and is particularly receptive around the sharp corners of the injector. Although it remains to be proven, this suggests that these regions play an important role in the thermoacoustic instability mechanism, in which the feedback between acoustic perturbations and hydrodynamic oscillations is influential. In order to examine this further, it will be necessary to examine the axisymmetric hydrodynamic mode, which is the one that locks into longitudinal waves in a combustor. This work is ongoing.

The overlap of the direct and adjoint global modes reveals the wavemaker region of the flow. This lies just upstream of the vortex breakdown bubble, as it does in the canonical vortex breakdown bubble at $\mathrm{Re} = 100$. This is the region that, if altered, has most influence on the growth rate and frequency of the first helical mode. Further results on a low Reynolds number flow ($\mathrm{Re} = 68$) in the same injector show the sensitivity of the first helical mode to changes in the inflow velocity and in the geometry of the injector. The former reveals that injection through the central stream has a strong stabilizing effect, which has already been verified experimentally. The latter reveals that the first helical mode is most sensitive to geometry changes at the corners of the injector.

The successful application of adjoint sensitivity analysis to the flow in a model gas turbine combustion chamber opens up new possibilities for injector design methodologies. It shows how the injector should be changed in order to change the stability or frequency of hydrodynamic oscillations. This gradient information can be included in optimization procedures (as it is already for steady flows) in order to systematically converge on optimal designs. The gradient information requires sensitivities and cannot be obtained by simply postprocessing nonlinear simulation results.

This study is on a non-reacting flow and much work remains. Nevertheless, it is a promising start for this new technique.

ACKNOWLEDGMENT

This work was supported by the European Research Council through Project ALORS 2590620 and was performed on Hector, the UK National Supercomputing Resource, and on the Darwin cluster of the University of Cambridge High Performance Computing Service.

REFERENCES

[1] Leibovich, S, 1978, "The structure of vortex breakdown", Annu. Rev. Fluid Mech. **10**, 221–246.

[2] Garcia-Villalba, Frohlich & Rodi, 2006, "Numerical simulations of isothermal flow in a swirl burner", ASME Turbo Expo GT2006-90764.

[3] Ruith, M. R., Chen, P., Meiburg, E. & Maxworthy, T., 2003, "Three-dimensional vortex breakdown in swirling jets and wakes: direct numerical simulation", J. Fluid Mech. **486**, 331–378.

[4] Gallaire, F., Ruith, M., Meiburg, E., Chomaz, J-M & Huerre, P., 2006, "Spiral vortex breakdown as a global mode", J. Fluid Mech. **549**, 71–80.

[5] Qadri, U., Mistry, D. & Juniper, M., 2013, "Structural sensitivity of spiral vortex breakdown", J. Fluid Mech. **720**, 558–581.

[6] Oberleithner, K., Stöhr, M., Imb, S. H., Arndt, C. M., Steinberg, A. M., 2014, "Formation and flame-induced suppres-

sion of the precessing vortex core in a swirl combustor: experiments and linear stability analysis", Comb. Flame (submitted)

[7] Midgley, K., 2005, "An isothermal experimental study of the unsteady fluid mechanics of gas turbine fuel injector flowfields", Ph.D. thesis, Loughborough University, U.K.

[8] Dunham, D., Spencer, A., McGuirk, J., Dianat, M., 2008, "Comparison of uRANS and LES CFD Methodologies for air swirl fuel injectors", ASME Turbo Expo GT2008-50278.

[9] Huerre, P. & Monkewitz, P., 1990, "Local and global instabilities in spatially developing flows", Ann. Rev. Fluid Mech. **22**, 473–537.

[10] Oberleithner, K., Sieber, M., Nayeri, C. N., Paschereit, C. O., Petz, C., Hege, G.-C., Noack, B. R., Wygnanski, I., 2011, "Three-dimensional coherent structures in a swirling jet undergoing vortex breakdown: stability analysis and empirical mode construction", J. Fluid Mech. **679**, 383–414.

[11] Juniper, M. P., 2012, "Absolute and convective instability in gas turbine fuel injectors", ASME Turbo Expo GT2012-68253.

[12] Juniper, M. & Pier, B., 2014, "The structural sensitivity of open shear flows calculated with a local stability analysis ", Europ. J. Mech. B, doi10.1115/1.4026604

[13] Chomaz, J.-M., 2005, "Global instabilities in spatially developing flows: non-normality and nonlinearity", Annu. Rev. Fluid Mech. **37**, 357–392.

[14] Hill, D. C., 1992 "A theoretical approach for analyzing the re-stabilization of wake", AIAA Paper 92–0067.

[15] Giannetti, F. & Luchini, P., 2007, "Structural sensitivity of the first instability of the cylinder wake", J. Fluid Mech. **581**, 167–197.

[16] Marquet, O., Sipp, D. & Jacquin, L., 2008 "Sensitivity analysis and passive control of cylinder flow" J. Fluid Mech. **615**, 221–252.

[17] Marquet, O. & Sipp, D., 2010 "Active, steady control of vortex shedding: an adjoint-based sensitivity approach." Seventh IUTAM Symposium on Laminar-Turbulent Transition IUTAM Bookseries **18**, 259–264.

[18] Barkley, D., 2006, "Linear analysis of the cylinder wake mean flow", Europhys. Lett. **75** (5) 750-756.

[19] Mettot, C., Sipp, D., and Bzard, H., 2014 "Quasi-laminar stability and sensitivity analyses for turbulent flows: Prediction of low-frequency unsteadiness and passive control," Phys. Fluids **26** (4) 045112.

[20] Fischer, P. F. & Kerkemeier, S. G. 2008 "Nek5000" `http://nek5000.mcs.anl.gov`

[21] Fischer, P. F., 1997 "An overlapping schwarz method for spectral element solution of the incompressible Navier–Stokes equations. J. Comp. Phys. **133**, 84–101.

[22] Maday, Y. & Patera, A. T. 1989 Spectral element methods for the Navier-Stokes equations. In *State-of-the-art surveys on computational mechanics* (ed. A. Noor), pp. 71–143. ASME.

[23] Berkooz, G. & Holmes, P. & Lumley, J. L. 1993 The Proper Orthogonal Decomposition in the analysis of turbulent flows. Annu Rev. Fluid Mech. **25** pp. 539–575.

[24] Sirovich, L. 1987 Turbulence and dynamics in coherent structures. Part I : Coherent structures. Quart. Appl. Math **45** pp. 561–571.

[25] Reynolds, W. C. & Hussain, A. K. M. F. 1972 The mechanics of an organized wave in turbulent shear flow. part 3. theoretical models and comparisons with experiments. Journal of Fluid Mechanics **54** (02), 263–288.

[26] Hecht, F. 2012 "New development in FreeFem++." J. Num. Math. **20**, 251–265.

[27] Tammisola, O., Giannetti, F., Citro, V. & Juniper, M. P. 2014 Second-order perturbation of global modes and implications for spanwise wavy actuation. *Journal of Fluid Mechanics* **755**, 314–335.

[28] Gikadi, J., Föller, S., and Sattelmayer, T., 2014 "Impact of turbulence on the prediction of linear aeroacoustic interactions: Acoustic response of a turbulent shear layer," J. Sound Vib. **333** (24) 6548–6559.

[29] Pralits, J. O., Brandt, L. & Giannetti, F., 2010 "Instability and sensitivity of the flow around a rotating circular cylinder" J. Fluid Mech. **650**, 513–536.

[30] Syred, N., 2006 "A review of oscillation mechanisms and the role of the precessing vortex core (PVC) in swirl combustion systems" Prog. Energy Comb. Sci. **32**, 93–161.

[31] Rees, S. & Juniper, M., 2010, "The effect of confinement on the stability of viscous planar jets and wakes", J. Fluid Mech. **656**, 309–336.

[32] Magri, L., See, Y.C., Ihme, M. & Juniper, M., 2014, "Multiple-scale adjoint sensitivity analysis of hydrodynamic / thermoacoustic instability in turbulent combustion chambers", Report of the Stanford CTR Summer Program (in print)